

## 1. Introduction

We report on the reconstruction of B decays in 2 non-charmed hadrons ( $B \rightarrow h^+h^-$ ) at CDFII. We describe the extraction and the optimization of the signal and the fit technique developed to obtain the preliminary measurements of:

$$\frac{BR(B_d \rightarrow \pi^+\pi^\pm)}{BR(B_d \rightarrow K^+\pi^\pm)}, A_{CP}^{dir}(B_d \rightarrow K^+\pi^\pm) \text{ and } \frac{f_s \cdot BR(B_s \rightarrow K^+K^\pm)}{f_d \cdot BR(B_d \rightarrow K^+\pi^\pm)}$$

The decays contributing to the  $B \rightarrow h^+h^-$  are:

- ✓  $B_d^0 \rightarrow K^+\pi^-$  and charge conjugate (BR =  $1.74 \cdot 10^{-5}$ )
- ✓  $B_s^0 \rightarrow K^+K^-$  and c. c. (unobserved)
- ✓  $B_d^0 \rightarrow \pi^+\pi^-$  and c. c. (BR =  $4.4 \cdot 10^{-6}$ )
- ✓  $B_s^0 \rightarrow K^-\pi^+$  and c. c. (unobserved)

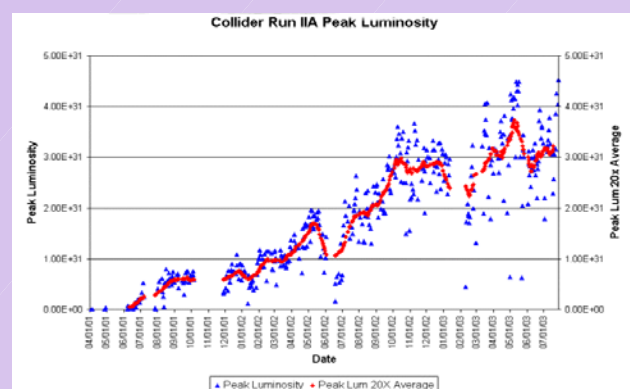
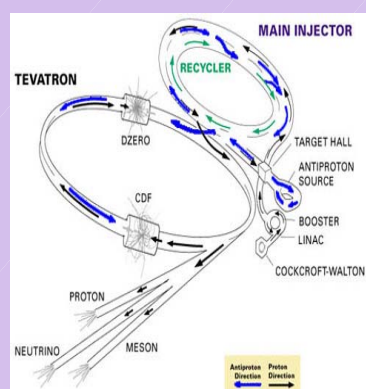
The decay amplitudes of these channels are directly connected with fundamental parameters of the CP violation theory within the Standard Model.

While the  $B_d$  channels are already widely studied at the B factories, the study of the  $B_s$  decays is unique to the Tevatron. The main difficulty of the analysis is to separate each contribution from the others. The preliminary results are promising: the  $B_d$  related measurements are consistent with the B-factories and a clean indication of  $B_s^0 \rightarrow K^+K^-$  decays is found.

# The CDFII detector at the Tevatron collider

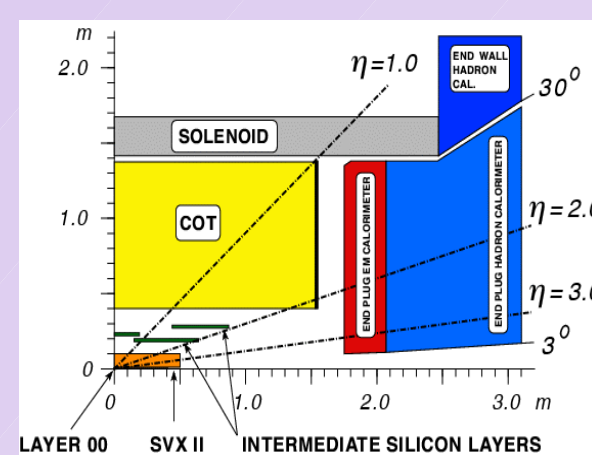
## 2. The upgraded Tevatron

Since the end of the first period of data-taking (RunI,1996) the Tevatron's accelerators have undergone a major upgrade. Several components were improved and two new machines were added. The Main Injector is an optimized injection stage for anti-protons production and the Recycler (still in commissioning) is an anti-protons storage and cooling ring. 36 bunches of protons circulate in the Tevatron against 36 bunches of anti-protons producing one collision every 396 ns at a center-of-mass energy of 1.96 TeV. Typical current peak luminosities range around  $4.0 \times 10^{31} \text{ cm}^{-2} \text{ s}^{-1}$



## 3. The CDFII detector

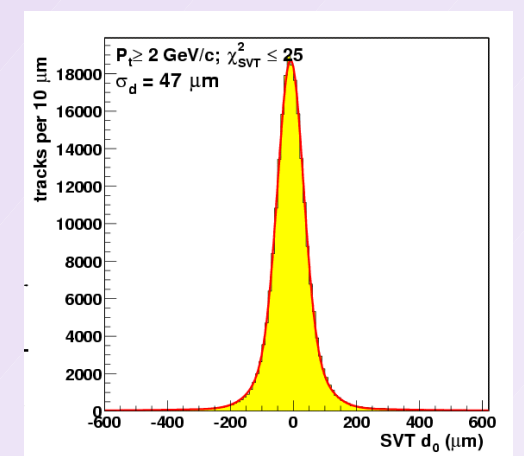
CDFII is a magnetic spectrometer surrounded by  $\sim 4\pi$  calorimetry with an external layer of muon chambers. The detector has been extensively upgraded to match the improved performances of the Tevatron. Only the solenoid, the central calorimeter and part of the muon systems are inherited from the Run I. The whole tracking system, the forward calorimetry, the trigger and DAQ systems are fully new. Part of the muon chambers is new and a Time-of-Flight detector has been added.



## 4. The tracking and the trigger on displaced vertices

The crucial devices for the present analysis are the tracking system and the trigger on displaced vertices. A silicon vertex detector and a drift chamber, both immersed in a 1.4T solenoidal field, sample the trajectories of the charged particles. 7 to 8 layers of double/single-sided Si sensors are installed at  $1.6 \text{ cm} < r < 28 \text{ cm}$  radii from the beam axis providing 3-D tracking with high ( $\sim 30 \mu\text{m}$ ) impact parameter resolution. The drift chamber samples 96 hits with  $\sigma(1/p_T) \sim 0.1\% \text{ c/GeV}$ , each hit encodes the  $dE/dx$  information which allows  $1.16\sigma$  of K to  $\pi$  separation for  $p_T > 2 \text{ GeV/c}$ .

The samples enriched in B flavor are collected through the new trigger on displaced vertices. This device reconstructs at trigger level 2-D silicon tracks with off-line quality on the impact parameter (IP) (right Figure). The IP information is used to select events with tracks displaced from the primary vertex.



## Analysis technique

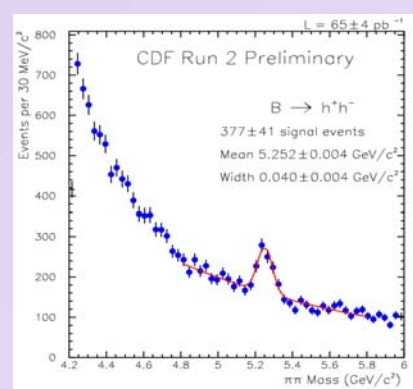
## 5. Description of the sample

The analysis is done on  $\sim 65 \text{ pb}^{-1}$  of data which pass the standard CDF data-quality requests. In all the data used the silicon tracker was on. The trigger selects events that have at least two oppositely-charged silicon tracks displaced from the primary vertex. Each track's  $p_T$  is required larger than  $2 \text{ GeV/c}$  and their scalar sum  $p_T(1) + p_T(2) > 5.5 \text{ GeV/c}$ . The displacement of the tracks is measured through their impact parameter (IP) which is  $100 \mu\text{m} < \text{IP}(\text{track}) < 1 \text{ cm}$ , additionally the transverse B decay-length  $L_{xy}(B)$  is required greater than  $200 \mu\text{m}$ . The transverse angular separation of the tracks is required to be  $20^\circ < \Delta\phi < 135^\circ$ . B's coming from the primary vertex are selected imposing  $\text{IP}(B) < 140 \mu\text{m}$ .

## 6. Signal extraction

A clear ( $\sim 377$  events) excess is already visible by confirming the trigger selections and by requiring some additional cuts. The main improvement is obtained by imposing the B to be "isolated" in the event.

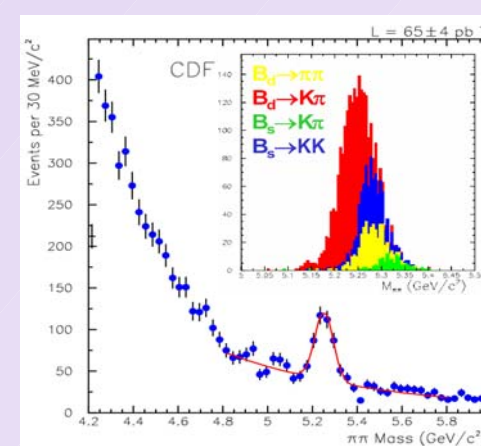
The 'isolation variable' is the ratio of the  $p_T(B)$  over the summed scalar  $p_T$ 's of all tracks lying in a cone whose axis is the B momentum and radius is 1 in the  $\eta - \phi$  metric. Isolation of the B is  $I(B) > 0.5$ .  $\pi\pi$  mass spectrum (right Figure).



The resolution on most CP-related measurements scales with the significance  $S/(S + \mathcal{B})^{0.5}$  as a function of the number of signal (S) and background (B) events. We optimize the selection cuts in order to maximize the significance. Signal S is a mixture (8:4:2:1) of the four decays  $B_d \rightarrow K\pi$ ,  $B_s \rightarrow KK$ ,  $B_d \rightarrow \pi\pi$ ,  $B_s \rightarrow K\pi$  generated by Monte Carlo.

Background B are real events sampled on the sidebands of the peak. We vary simultaneously the values of our cuts to find the optimal configuration which maximizes  $S/(S + \mathcal{B})^{0.5}$ :

- ✓  $\min p_T(1) + p_T(2) = 5.5 \text{ GeV/c}$ ;
- ✓  $\min[\text{IP}(1), \text{IP}(2)] = 150 \mu\text{m}$ ;
- ✓  $\min L_{xy}(B) = 300 \mu\text{m}$ ;
- ✓  $\max \text{IP}(B) = 80 \mu\text{m}$ ;
- ✓  $\min \text{Isolation}(B) = 0.5$



The resulting mass plot is shown  $\rightarrow$   
Yield:  $280 \pm 26$  events  
Mass:  $5.252 \pm .004$   
RMS:  $0.041 \pm .004$

### Experimental challenge

Owing to the limited performance of the CDFII detector in mass resolution and particle identification (PID), the contributions of all channels overlap into an unresolved mass peak. The main difficulty of the analysis is to separate each contribution from the others.

We exploit the combination of kinematics separation and particle identification.

Since our  $p_T$ 's are out of reach for the Time-of-Flight, we use PID provided by the specific ionization ( $dE/dx$ ) inside the drift chamber.

A 4-dimensional un-binned likelihood fit combines the information from kinematics and PID to obtain a statistical (rather than an event-by-event) separation.

## 7. Disentangling the components of the signal

Once chosen the  $\pi\pi$  mass assignment ( $M_{\pi\pi}$ ) for the 2 tracks, the shift between the reconstructed mass and the "actual" mass of the decaying particle depends just on  $M_{\pi\pi}$  and on the ratio  $p(1)/p(2)$ . Therefore the variables chosen for the fit are:

- ✓ the invariant mass of the 2 tracks with  $\pi\pi$  assignment  $M_{\pi\pi}$ ;
- ✓ the function  $\alpha$  of the 3-dimensional momentum unbalance:  
 $\alpha = [1 - p(1)/p(2)] \cdot Q(1)$   
where  $|p(1)| < |p(2)|$  and Q is the charge;
- ✓ the  $dE/dx - \langle dE/dx \rangle$  for each track.

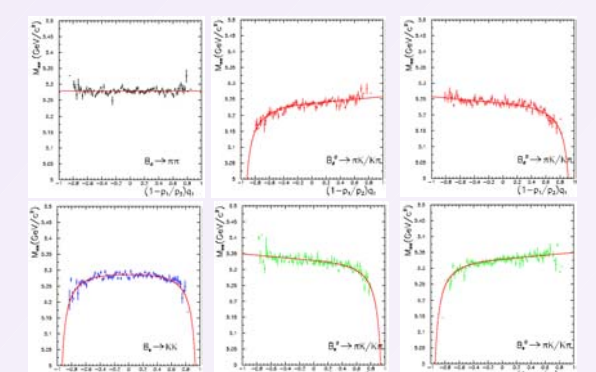
The likelihood function is :

$$L = \prod_i^{N_{\text{events}}} \left[ (1 - \text{bcgk}) \sum_j^{N_{\text{channels}}} f_j \cdot F_j^i + \text{bcgk} \cdot F_{BG}^i \right]$$

$$F_j = F_j(\alpha^i, M_{\pi\pi}^i, dE/dx(1)^i, dE/dx(2)^i) \text{ and } F_{BG} = F_{BG}(\alpha^i, M_{\pi\pi}^i, dE/dx(1)^i, dE/dx(2)^i)$$

The fit applied to the signal events returns the raw relative fractions which are then corrected for relative efficiencies and acceptances.

The Figure shows how  $M_{\pi\pi}$  and  $\alpha$  separate the 4 channels and discriminate between B and  $\bar{B}$  in the self-tagging modes.



## 8. Systematics and checks

The main sources of systematic uncertainties are:

- ✓ fluctuations of the  $dE/dx$  calibrations;
- ✓ uncertainty on the single-channel mass widths;
- ✓ modeling of the background;
- ✓ uncertainty on the  $B_s$  and  $B_d$  masses;
- ✓ uncertainty on the correction factors for relative efficiencies

Further checks exclude  $\Lambda_b \rightarrow p\pi$  contamination of the  $B \rightarrow h^+h^-$  signal.

$$\frac{BR(B_d \rightarrow \pi^+\pi^\pm)}{BR(B_d \rightarrow K^+\pi^\pm)} = 0.26 \pm 0.11(\text{stat}) \pm 0.055(\text{sys})$$

$$A_{CP}^{dir} = \frac{N(B_d^0 \rightarrow K^-\pi^+) - N(B_d^0 \rightarrow K^+\pi^-)}{N(B_d^0 \rightarrow K^-\pi^+) + N(B_d^0 \rightarrow K^+\pi^-)} = 0.02 \pm 0.15(\text{stat}) \pm 0.017(\text{sys})$$

$$\frac{f_s \cdot BR(B_s \rightarrow K^+K^\pm)}{f_d \cdot BR(B_d \rightarrow K^+\pi^\pm)} = 0.74 \pm 0.20(\text{stat}) \pm 0.22(\text{sys})$$

## 9. Conclusions

We reconstructed the first hadronic charm-less B decay in an hadronic environment with good S/N. We separated the contributions and we obtained exciting physics results: we have only a 15% (stat) error on the direct CP symmetry measurement in the  $B_d^0 \rightarrow K^+\pi^-$  and we have clean evidence for  $B_s^0 \rightarrow K^+K^-$  decays in just the first  $65 \text{ pb}^{-1}$  of data. The capability to combine  $B_d$  and  $B_s$  measurements allows CDFII to play an important role for the future CP violation measurements (see R. Fleischer, Phys.Lett.B 459 (1999) 306)